Indoor Localization of Persons in AAL Scenarios Using an Inertial Measurement Unit (IMU) and the Signal Strength (SS) from RFID Tags

Antonio R. Jiménez, Fernando Seco, Francisco Zampella, Jose C. Prieto, and Jorge Guevara

Centre for Automation and Robotics (CAR)
Consejo Superior de Investigaciones Científicas (CSIC)-UPM,
Ctra., Campo Real km 0.2, 28500 La Poveda, Arganda del Rey (Madrid), Spain
{antonio.jimenez,fernando.seco,francisco.zampella}@csic.es
http://www.car.upm-csic.es/lopsi

Abstract. This paper presents an indoor localization system that is based on the fusion of two complementary technologies: 1) Inertial integration and 2) RFID-based trilateration. The Inertial subsystem uses an IMU (Inertial Measurement Unit) mounted on the foot of the person. The IMU approach generates a very accurate estimate of the user's trajectory shape (limited by the drift in yaw). However, being a dead-reckoning method, it requires an initialization in position and orientation to provide absolute positioning. The IMU-based solution is updated at 100 Hz and is always available. On the other hand, the RFID-based localization subsystem provides the absolute position using the Received Signal Strength (RSS) from several long-range active tags installed in the building. Since the transmitted RF signals are subject to many propagation artifacts (reflections, absorption,...), we use a probabilistic RSS-to-Range model and a Kalman filter to estimate the position. The output of both IMU- and RFID-based subsystems are fused into one final position estimation by adaptively fitting the IMU and RFID trajectories. The integrated solution provides: absolute positioning information, a static accuracy of less than 2.3 m (in 75% of the cases) for persons at fixed positions, a smooth trajectory for moving persons with a dynamic positioning accuracy of 1.1 m (75%), a full 100% availability, and a real-time update rate of up to 100 Hz. This approach is valid for indoor navigation and particularly for Ambient Assisted Living (AAL) applications. We presented this system to the 2nd EvAAL competition ("Evaluating AAL Systems through Competitive Benchmarking": http://evaal.aaloa.org/) and our CAR-CSIC system was awarded with the first prize. A detailed analysis of the experiments during the competition is presented at the end of this paper.

Keywords: Inertial Navigation, RFID Positioning, Indoor Localization, Fusion Algorithms, Ambient Assisted Living, EvAAL competition.

S. Chessa and S. Knauth (Eds.): EvAAL 2012, CCIS 362, pp. 32–51, 2013.

1 Introduction

Two main research approaches are used in the indoor positioning problem: 1) solutions that rely on the existence of a network of receivers or emitters, some of them placed at known locations (beacon-based solutions), and 2) solutions that mainly rely on dead-reckoning methods with sensors installed on the person to be located (beacon-free solutions).

In the first approach (beacon-based), the positions are estimated by trilateration or triangulation from a set of measured ranges or angles, respectively. These methods are usually termed as Local Positioning Systems (LPS), or Wireless Sensor Networks (WSN), depending on the sensor configuration and processing approach. They use technologies such as ultrasound, short-range radio (WiFi, UWB, RFID, Zigbee, etc.) or vision [1].

The second approach (beacon-free or dead-reckoning) uses Inertial Measuring Units (IMU) to estimate the position of persons [2]. These IMU-based methodologies, often called Pedestrian Dead-Reckoning (PDR) solutions, can integrate the user step lengths and heading angles at each detected step, to estimate the user's position [3,4,5]; or, alternatively, integrate accelerometer and gyroscope readings of a foot-attached IMU (by strapdown INS mechanization [6]) to compute the position and attitude of the person [7,8,9].

IMU-based PDR solutions have the inconvenient of accumulating errors that grow with the path length (drift), while beacon-based solutions have limited absolute accuracy and coverage. The fusion of IMU-based PDR solutions with indoor absolute positioning has the potential to provide an accurate drift-free positioning solution. In this paper we propose an integrated IMU+RFID-based localization system. Section 2 presents the localization methodology, section 3 its evaluation at our site (CAR-CSIC) , and in section 4 we analyze in detail our experiences during the EvAAL competition.

2 The Localization System

The block diagram of the proposed indoor localization system is presented in Fig. 1. Two complementary but independent positioning methods are implemented: 1) IMU-based Positioning, and 2) RFID-based Positioning. The outputs of both systems $\mathrm{Pos}_{\mathrm{IMU}}$ and $\mathrm{Pos}_{\mathrm{RFID}}$, which contains the two-dimensional positioning coordinates of both approaches, are fused to generate the final position estimation: $\mathrm{Pos}_{\mathrm{Fused}}$. The next three subsections give details on each method.

2.1 The IMU-Based Dead-Reckoning Localization Method

Our method assumes that an IMU is installed on the foot of a person (the most reliable PDR method). The IMU contains 3 accelerometers and 3 gyroscopes, and provides the sensor acceleration ($\mathrm{m/s^2}$) and the angular rate (rad/s). An inertial navigation system (INS) algorithm is executed to integrate the accelerometer

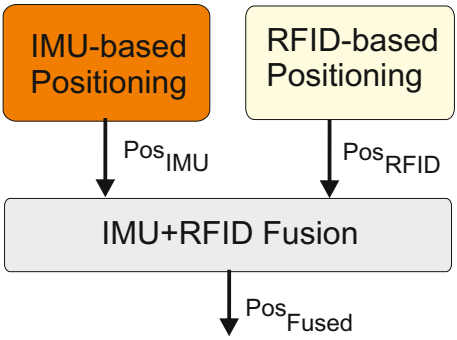

Fig. 1. Proposed positioning systems with "loose" IMU and RFID integration

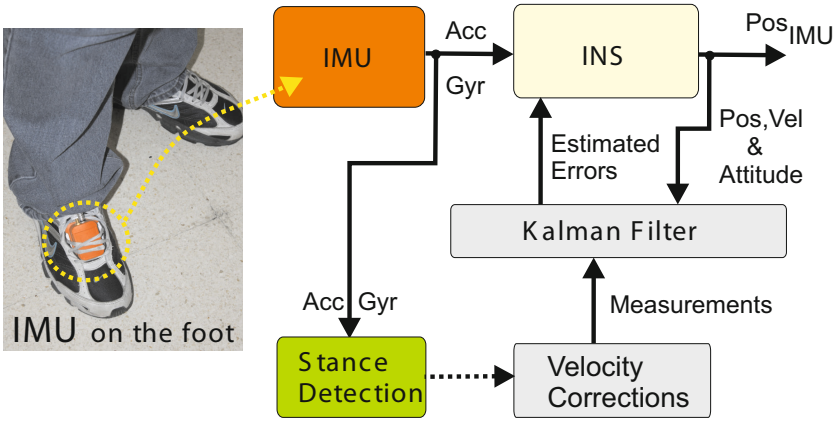

Fig. 2. Block diagram of the IMU-based dead-reckoning PDR method

readings into velocity and then into position, also the gyroscope angular rate readings are integrated to obtain the attitude of the IMU (i.e. Roll, Pitch and Yaw). See Fig. 2 for a simplified diagram of this approach.

The output of the INS needs to be corrected periodically or it will diverge quickly due to sensor drift. A very effective technique is the Zero Velocity Update (ZUPT), used every time that the foot is motion-less (stance phase), and consisting in updating the INS-estimated velocity with the "known" velocity of the foot at stance (zero velocity). This is a very effective way to reset the error in velocity of the INS.

A complementary Extended Kalman Filter (EKF), working with a 15-element error state vector [7,9], compensates position, velocity and attitude errors of the INS solution, as well as the IMU biases. Our methodology is valid for any kind of motion (forward, lateral or backward walk), and does not require a specific off-line calibration of the user gait.

2.2 The RFID RSS-Based Absolute Localization Method

It is assumed that an RFID reader is carried by a person and several active tags are fixed at known locations in the building. The RFID reader provides the Received Signal Strength (RSS) of each tag. A RSS-to-range model is used to estimate the expected range between the reader and a particular tag (also its uncertainty). Then, an EKF integrates all range measurements into a position fix (dynamic trilateration). See Fig. 3 for a simplified diagram of the RFID-based location method.

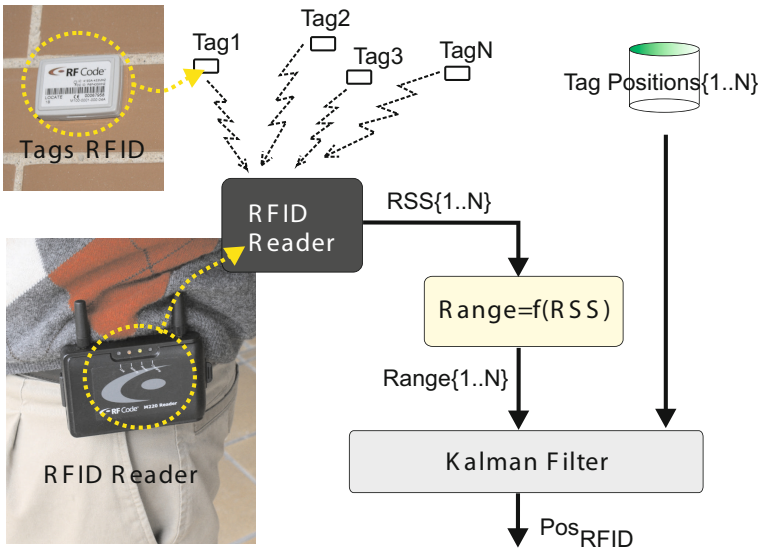

Fig. 3. Block diagram of the active RFID-based absolute positioning system

The path-loss model that we use to transform from RSS to distance, d, (maximum likelihood estimate) is given by

$$d = d_0 \cdot 10^{\frac{\mathrm{RSS}_0 - \mathrm{RSS}}{10 \cdot p}}, \tag{1}$$

where RSS_0 is a mean RSS value obtained at a reference distance d_0, and p is the path loss exponent (we experimentally found these values: $\mathrm{RSS}_0 = 60$, $d_0 = 1$ m and $p = -2.3$).

The standard deviation of the estimated distance, σ_d, is needed by the Kalman filter as an indication of the belief we have on the modeled range value. It is

$$\sigma_d = \sigma_{\mathrm{RSS}} \cdot \frac{\ln(10) \cdot d}{-10 \cdot p}, \tag{2}$$

where σ_{RSS} is the RSS standard deviation in dB. This sigma model is proportional to distance, giving low standard deviation values at short ranges (low uncertainty) and viceversa.

The Kalman filter uses a 4-component state vector (X) that contains the 2-D position and velocity, i.e. $X = [\mathrm{Pos}_{\mathrm{RFID}}(x), \mathrm{Pos}_{\mathrm{RFID}}(y), \mathrm{Vel}_{\mathrm{RFID}}(x), \mathrm{Vel}_{\mathrm{RFID}}(y)]$. In order to predict the next state, X^-, we use a movement model that relates the current state with its predicted state as $X^- = A \cdot X$, which uses a constant velocity model as detailed in matrix A:

$$A = \begin{bmatrix} I_{2x2} & \Delta T \cdot I_{2x2} \\ 0_{2x2} & I_{2x2} \end{bmatrix}, \tag{3}$$

being ΔT the sampling interval, I_{2x2} a 2 by 2 diagonal matrix, and O_{2x2} a 2 by 2 matrix of zeros.

We use a difference-in-range measurement model to feed our Kalman filter. This measurement is $\Delta d_i = d_i - d_i^-$, being Δd_i the differences between the measured range, d_i, to the i-th tag obtained with equation 1, and being d_i^- the computed range between the current estimation and the position of i-th tag, i.e.

$$d_i^- = [(\mathrm{tag}_i(x) - \mathrm{Pos}^-_{\mathrm{RFID}}(x))^2 + (\mathrm{tag}_i(y) - \mathrm{Pos}^-_{\mathrm{RFID}}(y))^2]^{0.5}. \tag{4}$$

After a first order linearization of the measurement equation, we obtain matrix H,

$$H = \begin{bmatrix} \frac{\mathrm{tag}_1(x) - \mathrm{Pos}^-_{\mathrm{RFID}}(x)}{d_1^-} & \frac{\mathrm{tag}_1(y) - \mathrm{Pos}^-_{\mathrm{RFID}}(y)}{d_1^-} & 0 & 0 \\ \frac{\mathrm{tag}_2(x) - \mathrm{Pos}^-_{\mathrm{RFID}}(x)}{d_2^-} & \frac{\mathrm{tag}_2(y) - \mathrm{Pos}^-_{\mathrm{RFID}}(y)}{d_2^-} & 0 & 0 \\ \cdots & \cdots & \cdots & \\ \frac{\mathrm{tag}_N(x) - \mathrm{Pos}^-_{\mathrm{RFID}}(x)}{d_N^-} & \frac{\mathrm{tag}_N(y) - \mathrm{Pos}^-_{\mathrm{RFID}}(y)}{d_N^-} & 0 & 0 \end{bmatrix}, \tag{5}$$

that is used to compute the Kalman gain $K = P^- \cdot H^T \cdot (HP^-H^T + R)$, and this to update the state estimation of the EKF with $X = X^- + K \cdot \Delta d_i$, being R the system model covariance matrix and P^- the covariance of the predicted state estimation that is a 4 by 4 matrix. Finally, the covariance of the estimation after the measurement update is $P = (I_{4x4} - K \cdot H) \cdot P^-$.

This subsection has presented a long-range RFID strategy for localization. Alternatively we could have implemented a passive short-range RFID strategy based on cell-based or proximity positioning algorithms. However we prefer our long-range RFID solution since it is a general purpose approach. It can be easily adapted to provide location-awareness in large buildings simply by putting the tags apart from each other (lowering the tag density).

In the implementation presented in this paper, we use long-range RFID technology for a quite small space (approx. 100 m^2). Consequently it is expected that almost all tags will be detectable from any position in the AAL scenario. In order to obtain enough accuracy a high tag density guaranties that the person to be located is always close to some of the tags. We use all distances or RSS data available for positioning, however our algorithm (see eq. 4) weights short distances (strong RSS) much more than large distances (weak RSS). If the person is close enough to a tag (less than 1 m), the system performs a kind of cell-based positioning (the information from 1 tag is predominant over the others). This

way, the positioning accuracy is expected to be about 1 m, which is better than the typical accuracy (2-3 meters) using distant or a low density of tags.

2.3 The Integrated IMU+RFID Positioning Method

The fusion method that we propose is based on the superposition of the smooth but not well-oriented IMU trajectory ($\mathrm{Pos}^{i}_{\mathrm{IMU}}$) over the noisy but well-aligned RFID-based trajectory ($\mathrm{Pos}^{i}_{\mathrm{RFID}}$). This superposition is made basically by iteratively fitting long sections of the IMU trajectory with the same temporal section of the RFID-based trajectory. The fitting process is stated as a least square minimization problem (Downhill Simplex method), where 3 variables are optimized: the offsets along X and Y axis (ΔX, ΔY), and the orientation mismatch between the IMU and RFID trajectories (θ). These parameters represent the misalignment of the IMU trajectory with respect the RFID trajectory.

Once we have a first estimation of the misalignment between the IMU and RFID trajectories (ΔX, ΔY, θ), the output of the fused solution is just a reoriented version, according to the misalignment parameters, of the IMU-based positioning solution. In this way we can provide a real-time positioning solution at a rate up to 100 Hz. Since the IMU suffers from drift we can not rely the fused solution on the initial misalignment parameters, then the fit is repeated once in a while at a low rate.

The rate at which we update the misalignment parameters (ΔX, ΔY, θ) is not critical. For example a fit can be performed at a fixed time interval, e.g. every 60 s, or when enough person's movement is detected. For example, the minimum amount of movement required to perform a new fit can be traveling a distance of at least 4 times the accuracy of the RFID-based positioning system (we use 10 meters as threshold).

Note that at the very beginning, when no fitting is still done and no misalignment parameters are known, the fused solution only uses the RFID data ($\mathrm{Pos}_{\mathrm{RFID}}$).

3 Evaluation at CAR-CSIC

We have tested the system in an indoor area (Research Lab) of 80 square meters, at the Center of Automation and Robotics (CAR-CSIC) (see Fig. 4). This area was selected since it is similar in size to an apartment in Ambient Assisting Living (AAL) applications.

3.1 Complexity of the Installation

Infrastructure in the Building. The building has to be equipped with several active RFID tags placed on the walls or the furniture. A total of 24 tags were installed. The installation process is very fast, but the position of the tags must be annotated in an existing floor plan which provides the coordinate

Fig. 4. Lab used for tests (CAR-CSIC)

reference frame for the localization. The used tags are model M100 from RFCode (www.rfcode.com), which are battery-powered RF transmitters operating in the 433 MHz radio band. Every tag broadcasts its unique ID and a status message at a periodic rate (1 Hz).

Sensors Installed on the Person. The user must carry an IMU on the foot and an RFID reader on its waist. We use a commercially available IMU, model MTi from Xsens Technologies (www.xsens.com), which weights 50 grams. It is configured to provide inertial data at 100 Hz. The RFID reader is model M220 from RFCode, which is a light-weight (160 g) portable battery-powered device. This RFID reader is able to detect the active tags at long distances; the typical maximum detection range is about 25 meters, and in our indoor experiments the reader detects tags at a distance of 12 meters in 75% of the cases.

Computation Platform. We use a netbook computer to execute the location algorithms and to make a graphical representation in real-time. The computer in our current prototype is carried by the user, and sensors are connected to it by USB. In the near future, we plan to use a more wearable platform (tablet or smartphone) to read the internal sensors (Accelerometers, Gyroscopes and WiFi) or any additional wireless external sensors (IMU or RFID reader). The tablet/smartphone could also perform the data processing to estimate the localization of the person.

3.2 Tracking with the IMU Subsystem

The estimation of the shape of the trajectory with an IMU is very reliable at short-term and it is always available. It accumulates an error of about 1% of

the Total Travelled Distance (TTD), i.e. if we start at a given position and end at the same place after 100 meters of walk, the expected positioning error will be about 1 m. However, the main inconvenient is that the absolute position and orientation of the trajectory remain unknown unless they are provided at initialization. The path at the top of Fig. 5 is a typical IMU-based estimation, where small dots represent the detected foot stances (notice the error in the orientation of the trajectory).

3.3 Tracking with the RFID Subsystem

This absolute positioning method has typical positioning errors of about 2.3 m (75th percentile). This limitation, common to most RSS-based positioning methods (fingerprinting can obtain better results but at a cost of a systematic calibration), makes difficult to give accurate tracking results at apartment-size scale. However, the use of a higher density of tags helps in the accuracy that can be obtained, specially if tags are placed close to the site where the person is prone to pass by. At shorter reader-to-tag distances the uncertainty on the range is lower (eq. 4) so position estimations are more accurate. See the middle trajectory in Fig. 5 to get an idea of the tracking performance obtained.

3.4 Tracking with the Fused IMU-RFID System

The availability of the fused solution is 100% because the IMU is always providing inertial data and also the RFID system in apartment-size spaces is always available. The static positioning accuracy for a person at a fixed location is similar to the RFID alone system (2.3 meters, 75%). However, if the person moves from time to time to a different area, the generated trajectory and the fusion process helps to improve the accuracy in positioning (down to 1.1 m, 75%). The histograms in Fig. 6 show the distribution of the measured positioning errors for the RFID and fused estimations. This improvement is specially effective with long paths and diversified routes because in that case the systematic positioning errors that appear at certain areas with the RSS-based method are averaged. In the bottom of Fig. 5 it can be seen that the fused trajectory is smooth and well-positioned over the ground-truth path.

3.5 Regions of Interest Detection

Sometimes symbolic positioning provides more meaning than coordinate positioning. The detection of particular Regions of Interest (RoI) where the user can be located is very important in AAL (e.g. to be in the Kitchen, bathroom or bedroom).

In our symbolic location tests we use a polygon to define each particular RoI. Whenever the physical location estimate $\mathrm{Pos}_{\mathrm{Fused}}$ is inside the area defined by the polygon, the system indicates that the person is located in that RoI. We have defined 6 RoI as depicted in Fig. 7a. The success in the identification of the correct RoI is shown in Fig. 7b, in which 7 RoI are visited sequentially, stopping 30 s in

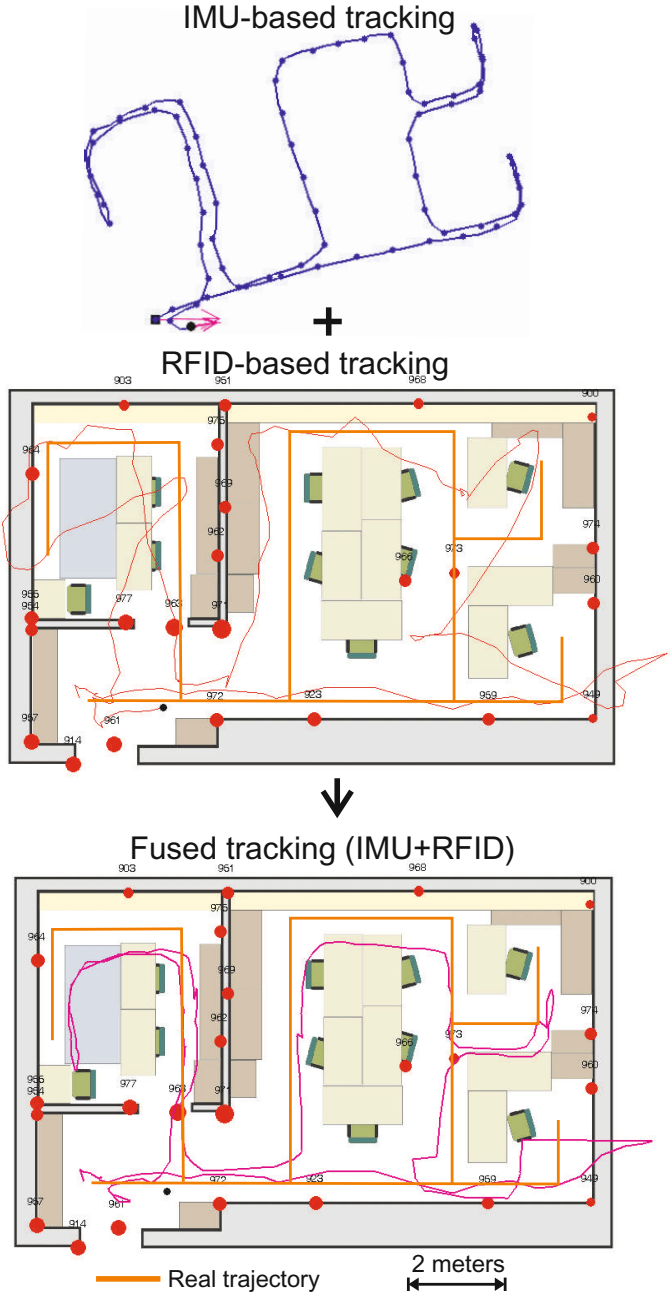

Fig. 5. Tracking with the IMU-based method (top), with the RFID-based method (middle), and with the Fused IMU+RFID method (bottom). Red circles represent the RFID tags positions with their sizes proportional to the RSS received from them at a given instant. The ground truth is marked in the middle and bottom plot with orange straight lines.

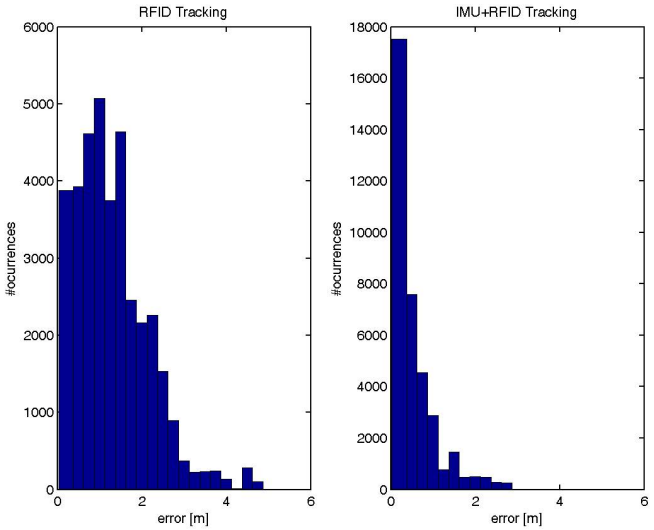

Fig. 6. Positioning error Histograms for the RFID and fused estimations

each area, with 10 s transition time employed to move from one RoI to the next. We did two different tests (plotted in Fig. 7b), and concluded that the system does not have a perfect detection rate, but detects many of the regions of interests.

The detailed performance statistics indicate that when the user is in any of the six RoIs, the system estimates the correct region in 65% of the cases. The system did not generated any region detection, when it actually was in one of them, in 33.8% of the cases. However only in 1.2% of the cases the systems indicates a wrong region. On the other hand, when the user was not in any of the regions of interest, the system correctly detected that state in 44.5% of the cases, so in 55.5% of the cases a false alarm is generated indicating that the user is in a region when actually is not.

4 Performance at EvAAL

We presented this system to the 2nd 2012 EvAAL competition ("Evaluating AAL Systems through Competitive Benchmarking": http://evaal.aaloa.org/), which is a competition to test AAL solutions in two different specialities: 1) tracking a person inside an apartment and 2) doing action recognition. We participated in the tracking and localization section, which had a total of eight competitors from countries all around the world.

The evaluation of our system was performed in the morning of the 3th of July 2012, between 8:30 and 11:30, in the Living Lab of the Polytechnic University of Madrid, Spain. This system was the first one to be evaluated in the localization track. Next subsections will give some details about this evaluation.

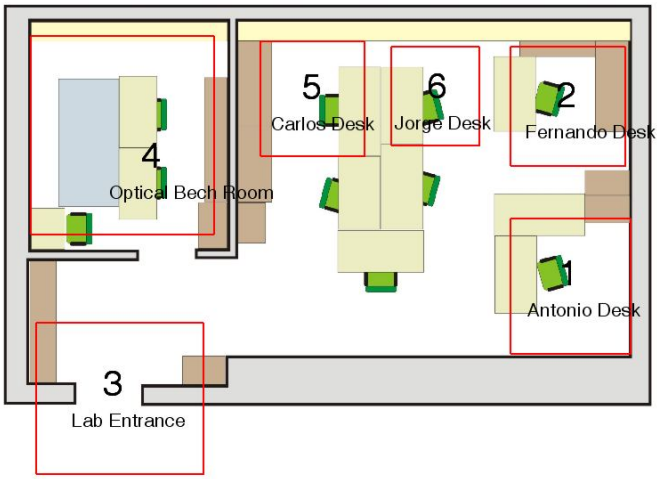

a)

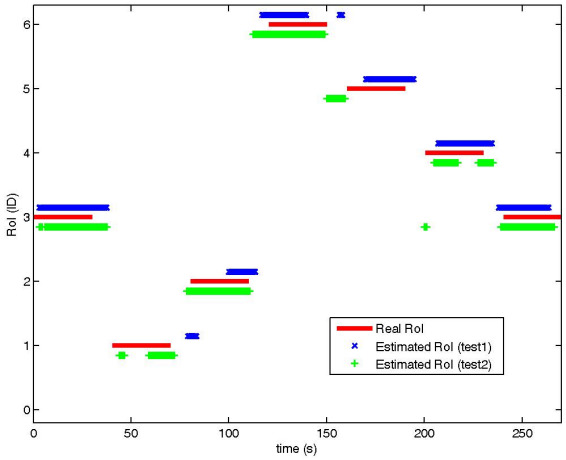

b)

Fig. 7. RoI detection tests. a) Six selected RoIs, b) Identification results for two different tests (ground truth in red).

4.1 Installation of RFID Tags and Sensors

We installed 30 RFID tags in the Living Lab. The CAR team had previously defined where to locate each tag using the map information available for competitors. One person stuck the 30 tags using BlueTack® sticky gum in 6 minutes and 39 seconds. The distribution of the tags can be seen in figure 8, the vertical position of all tags was approximately the same (about 1 meter). The exact position of the tags once installed was not measured by any measuring device, they were just placed by hand approximately at the locations previously

defined (red circles in the map in figure 8). A probable positioning error of about 20 cm is not significant neither important for our system's accuracy.

The installation of the sensors on the actor was simple but somehow tricky. The RFID reader was placed on the actor's waist easily, but the IMU sensor was a bit more complicated since the actor used sandals with a very reduced surface to attach the sensor. Finally we fixed it with double-side sticky foil and secured it with some electrical tape. See figure 9 for details. The user has also to carry with him the netbook computer where the localization algorithms are executed. In order to facilitate the transportation we initially put the computer inside a back pack. Finally, in order to avoid a lower processing power mode of the computer when folded in the bag, the actor carried the computer close to his hip keeping the arm straight to diminish muscle stress due to computer's weight.

It is important to mention that after installing the sensors in this Living Lab, we did not perform any calibration of the RFID subsystem. In principle the RSS-to-distance model presented in section 2.2 was calibrated for the CAR-CSIC building, but this model is a general purpose one that should not be significantly affected by operating in different buildings made using typical construction methods. We do not need a very precise and particular calibration, as opposite to other methods such as fingerprinting. So all the test at EvAAL were performed using the same model as explained in section 2.2 (i.e. $\mathrm{RSS}_0 = 60$, $d_0 = 1$ m and $p = -2.3$).

4.2 Generated Data

Our localization algorithm generated, as required for the competition, the position information and the detected areas of interest at a 2 Hz update frequency. The method used to transfer the information to the EvAAL server was to create a TCP/IP socket using port 4444 and transmitting the information to the local IP address '127.0.0.1'. The computer had installed a socket receiver (provided by the EvAAL team) that finally retransmits it to the EvAAL server. The format used to transmit the information consists of a header indicating the competitors identification name followed by the 2D position, the time stamp and a variable field with none, one or several areas of interest, i.e.:

<Competitors ID> <X position in meters> <Y position in meters> <Posix time in milliseconds> <AOI-Areas of Interest (1 o several integers)>.

See Fig. 10 for an example of real data transmitted during the competition. Note in this example that at the begining the user is close to the lab's table and no region of interest (RoI) is transmitted, but after that it detects to be on RoI 31 that is a subregion contained in RoI number 3. In figure 11 it can be seen all the RoIs that had to be detected, as defined by the EvAAL team.

Apart from the information previously described which is transmitted in real-time, the CAR system also generates some log files (saved in real-time during each session test) containing much more data of interest. At the end of the evaluation we made available to the EvAAL team two files: 'logfile_2012.7.3_11.15.57.511.mat' and 'logfile_2012.7.3_10.19.25.904.mat' (*.mat

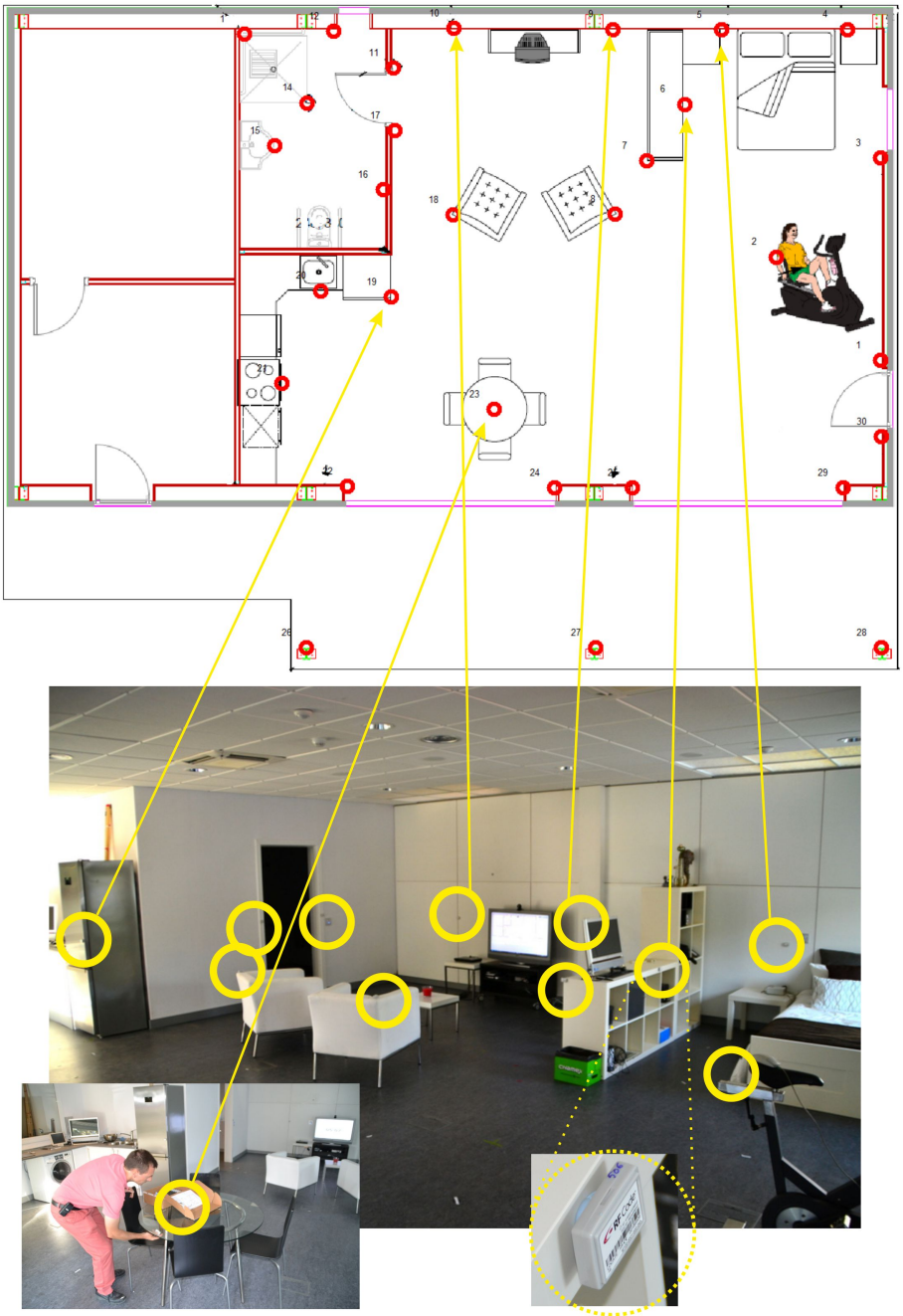

Fig. 8. Installation of 30 RFID tags in the Living Lab of the Polytechnic University of Madrid, Spain

Fig. 9. Installation of the sensors on the actor. The IMU on one of the sandal's strips and the RFID reader on the waist belt.

```
CAR-CSIC 5.043 3.192 1341313375147
CAR-CSIC 5.043 3.192 1341313375647
CAR-CSIC 4.832 2.63 1341313376147
CAR-CSIC 4.832 2.63 1341313376647
CAR-CSIC 3.761 3.71 1341313377147
CAR-CSIC 3.761 3.71 1341313377647
CAR-CSIC 4.072 5.097 1341313378147 3  31
CAR-CSIC 4.072 5.097 1341313378647 3  31
CAR-CSIC 4.969 4.149 1341313379147 3  31
CAR-CSIC 4.969 4.149 1341313379647 3  31
CAR-CSIC 5.326 4.94 1341313380147 3  31
CAR-CSIC 5.326 4.94 1341313380647 3  31
CAR-CSIC 5.663 4.533 1341313381147 3  31
CAR-CSIC 5.663 4.533 1341313381647 3  31
CAR-CSIC 6.623 4.194 1341313382147 3
CAR-CSIC 6.623 4.194 1341313382647 3
CAR-CSIC 6.239 5.858 1341313383147 3
CAR-CSIC 6.239 5.858 1341313383647 3
```

Fig. 10. Example of data transmitted from the CAR-CSIC system to the EvAAL server

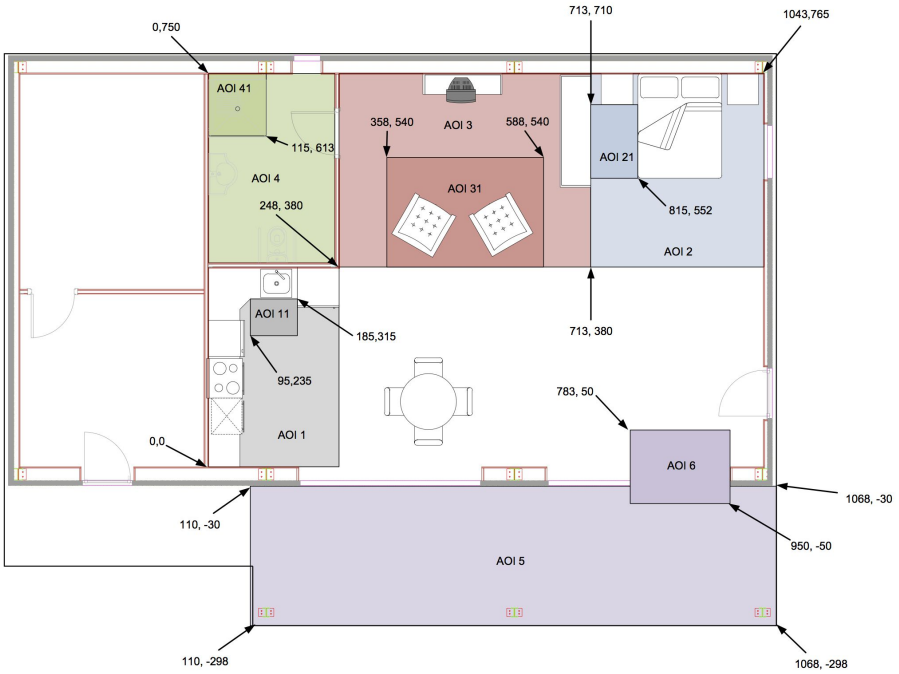

Fig. 11. Regions of Interes (RoI) defined to be detected al the Living Lab

is a Matlab file format) that can be post processed to evaluate other algorithms or approaches. These files contain, among other information, the following data:

1. The 3D (X-Y-Z) position coordinates of the fused RFID+IMU estimation.
2. The 3D (X-Y-Z) position coordinates of the IMU alone estimation.
3. The 2D (X-Y) position coordinates of the RFID alone estimation.
4. The Orientation of the person (Yaw angle with respect to the North).
5. Region-of-Interest (RoI) Identity in which the user is believed to be located.
6. User's foot activity (Walking or Still) and Step length (SL).
7. Raw Sensor data:
   - The sensor acceleration (m/s^2) provided by the 3 accelerometers.
   - The angular rate (rad/s) provided by the 3 gyroscopes.
   - Magnetic field (a.u.) provided by 3 magnetometers.
   - The Received Signal Strength (RSS) of tags provided by the RFID reader.

4.3 The Different Tests and the Obtained Results

There were three different parts during the evaluation period: 1) System installation in the Lab, 2) Tracking and Localization tests, and 3) Removing the installation. For each of the three parts a maximum time-slot of one hour

was allowed. Our system was installed and uninstalled in just a few minutes (less than 10 minutes in total), so we obtained the maximum score in the 'Installation Complexity' metric. The second part ('Tracking and Localization tests') consisted of three different phases: a) Location of a moving person inside the lab, b) Similar to the latter but with another disturbing person walking around, and c) detection of areas of interest. Each of these phases was repeated twice, and the best of the two tests was used to compute the final score.

The tracking accuracy was measured as the 75% percentile error of the Euclidean distance between the estimated position and the ground-truth reference, as computed in section 3. Errors below 0.5 m are scored 10 points; scores are given between 10 and 4 for errors from 0.5 m to 2 m; and finally scores goes linearly down from 4 to 0 for errors between 2 and 4 meters. Our system obtained and average localization accuracy of 7.9 which corresponds with a 75% error of 1.1 meters. This performance is exactly the same that we obtained in our own tests at CAR-CSIC Lab as presented before. Some of the estimated trajectories can be seen in figure 12.

The RoI test obtained a 6.3 score which is again similar to the score we obtained in our premises.

The total computed metrics are shown in Table 1, where it can be seen that the availability of the system was 82.1%, the user acceptance received a 6.56 score, and the interoperability of the system obtained a 6.81 score. The total score of the system was **7.70**, which was the maximum of the eight competitors at EvAAL, so the CAR-CSIC system was the winner of this second EvAAL competition.

Note that we did not obtain a 100% availability, even when our system is by definition a 100% available (the IMU always provides data at a 100 Hz rate and the RFID tags are always visible in this small localization area). After the competition we analyzed, looking into the log files, any kind of problems during the data transmission. We verified that we correctly transmitted data packets every 500 ms (2Hz), although the clock that we used to decide when to transmit the next package was the IMU clock. The IMU clock accumulated 8.71 seconds of delay with respect to the PC clock in a test that lasted for 839.7 seconds. So the IMU's clock was 1.1% slower than the PC's clock. Nevertheless this was not the cause of the 81% availability since a 1.1% slower clock would have cause a 98.9% availability. We finally found that the wireless transmission from the CAR PC to the server suffered some random delays that caused some time jitter (significantly larger than 0.25 s), causing the server to ignore approximately one data packet of five intents (80%). In figure 13 we can clearly see that instead of receiving each packet with a 500 ms separation, we get significant undesirable delays around a mean value of 500 ms.

4.4 Lessons Learned and Future Improvements

Although our system was a research prototype, and we already knew that it was not very wearable (the need to carry a netbook computer and a tethered IMU), it did not receive a bad score in user acceptance metric. The reason of

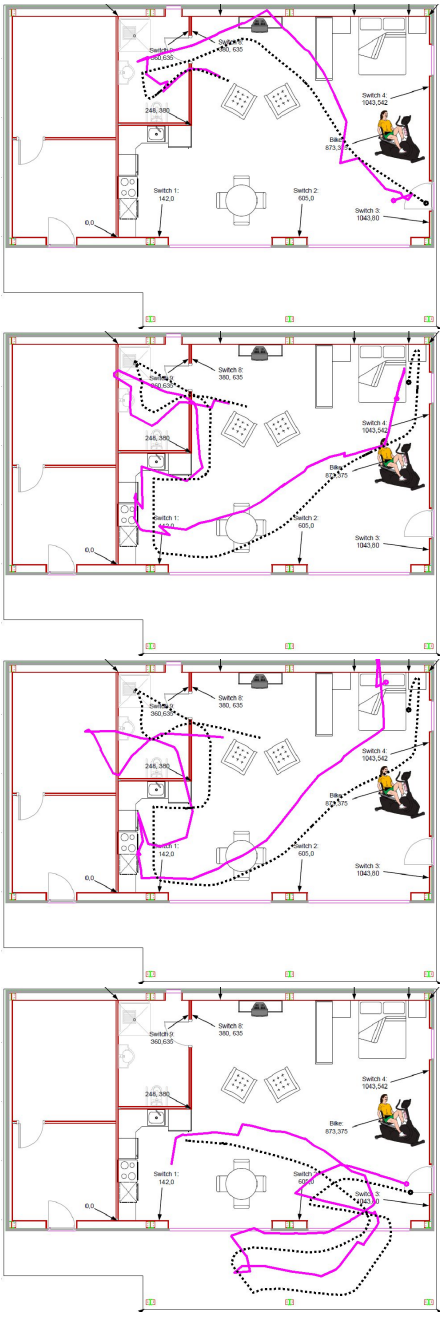

Fig. 12. Some of the individual path estimations during the tracking tests at the EvAAL Living Lab. The discontinuous line is the reference and the solid line is our estimation. A big dot on those trajectories represents the starting point. The scores for these tests were: 8.9, 8.02, 5.89 and 8.68 from top to bottom, respectively.

Table 1. Detailed score of CAR system

Metric	Weight	Score
Accuracy	0.25	7.57
- Tracking Location		8.8
- RoI detection		6.3
Availability	0.2	8.21
Installation Complexity	0.15	10.0
User Acceptance	0.25	6.56
Interoperability	0.15	6.81
Final score		**7.70**

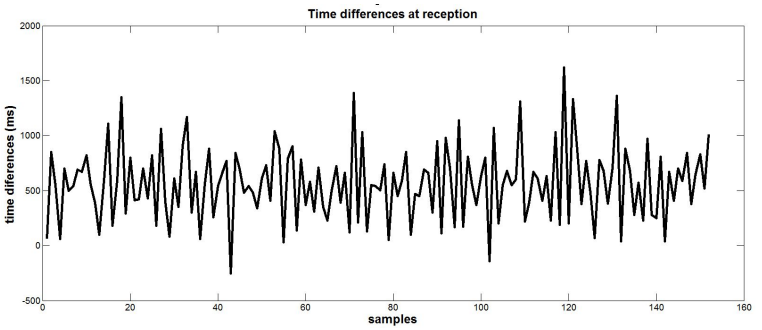

Fig. 13. Detected jitter at the reception of each data packet. This is the cause of the 81% availability of the system.

this, we believe, is that the localization concept proposed by us is in reality quite wearable. In fact we plan for a near future to have the system implemented on a smartphone, making use of its internal sensors (accelerometer and gyroscopes), as well as, their capacity to read RFID/WiFi/Bluetooth signals. With this hardware we can create a similar hybrid localization solution (IMU+RF) that only requires the use of a smartphone carried by a person, and some small RFID/WiFi/Bluetooth tags stuck on the walls of the smart home. A challenge will be to process the IMU signals coming from the smartphone, since in that case a Zero Velocity Update (ZUPT) can not be done.

Our system, as described before, is able to read the Earth magnetic field since our IMU has three magnetometers. With this information we could have better estimated the orientation of the person, but we decided not to use that information because in general magnetic information is not reliable in indoor environments (due to the presence of metallic objects, magnets, motors, and some other magnetic field disturbers). So it is commonly admitted that magnetic information can be beneficial outdoors, but indoors it could be detrimental [10]. When we analyzed, after the competition, the orientation estimated with the

magnetic compass and compared it to the actual orientation, we saw that the orientation errors were frequent in the Living Lab, so we took a good decision not making use of it.

Our system could have also been improved if the map information (position of doors, walls, and so on) of the living Lab had been used. Map information could have avoided the generation of localization points outside the living lab space, and also it would have improved the RoI correct detection rate. Additionally, our system was able to read the switch messages provided by the building when the user switch on or off a lamp, but we finally decided not to use it since the correction methodology was not well studied and debugged at the time of the competition. So, in conclusion, we get satisfied by the results that we obtained at this competition, but we think that there is room to improve our results a little bit more with a future prototype that would use a more wearable device, as well as the information from a floor map and the user's actions.

5 Conclusion

We have presented one localization system integrating two independent but complementary positioning methods: 1) IMU-based Positioning, and 2) RFID-based Positioning. The output of both systems Pos_{IMU} and Pos_{RFID}, which contains the two-dimensional positioning coordinates of both approaches, are fused to generate the final position estimation, $\text{Pos}_{\text{Fused}}$. This estimate gathers together the benefits of each individual solution: absolute estimation, quite smooth tracking, full availability and real-time update rate. A complete evaluation is performed in two labs: CAR-CSIC and the Living Lab of UPM. Over an area of 100 square meters we obtained an accuracy of 1.1 m in %75 of the cases, and a capability to detect RoI of 65%. the system also had excellent installation times and good user acceptance. The described system was the winner of the second edition of the 2012 international EvAAL competition.

References

1. Hightower, J., Borriello, G.: Location Systems for Ubiquitous Computing. Computer 34(8), 57–66 (2001)
2. Collin, J.: Investigations of Self-Contained Sensors for Personal Navigation. PhD thesis (2006)
3. Stirling, R.: Development of a Pedestrian Navigation System Using Shoe Mounted Sensors. PhD thesis, University of Alberta (2004)
4. Ladetto, Q.: J Van Seeters, S Sokolowski, Z Sagan, and B. Merminod: Digital Magnetic Compass and Gyroscope for Dismounted Soldier Position and Navigation. Sensors & Electronics Technology Panel, NATO Research and Technology Agency Sensors, pp. 1–15 (2002)
5. Jiménez, A.R., Seco, F., Prieto, J.C., Guevara, J.: A comparison of Pedestrian Dead-Reckoning algorithms using a low-cost MEMS IMU. In: 2009 IEEE International Symposium on Intelligent Signal Processing, pp. 37–42. IEEE (August 2009)

6. Chatfield, A.: Fundamentals of High Accuracy Inertial Navigation. AIAA, American Institute of of Aeronautics and Astronautics (1997)
7. Foxlin, E.: Pedestrian tracking with shoe-mounted inertial sensors. IEEE Computer Graphics and Applications, 38–46 (December 2005)
8. Feliz, R., Zalama, E., García-Bermejo, J.G.: Pedestrian tracking using inertial sensors. Journal of Physical Agents 3(1), 35–43 (2009)
9. Jiménez, A.R., Seco, F., Prieto, J.C., Guevara, J.: Indoor Pedestrian Navigation using an INS/EKF framework for Yaw Drift Reduction and a Foot-mounted IMU. In: WPNC 2010: 7th Workshop on Positioning, Navigation and Communication, vol. 10, pp. 135–143 (2010)
10. Jiménez, A.R., Seco, F., Zampella, F., Prieto, J.C., Guevara, J.: Improved heuristic drift elimination with magnetically-aided dominant directions (MiHDE) for pedestrian navigation in complex buildings. Journal of Location Based Services 6(3), 186–210 (2012)